LONG DISTANCE HYPERSPECTRAL IMAGING PANORAMA OVER THE DUNITIC TRANSITION ZONE / MOHO CONTACT OF THE OMAN OPHIOLITE: IN SITU TESTING AND SCIENTIFIC ASSESSMENT OF A NEW ADVANCED SENSOR.

P.C. Pinet[1], Y.D. Daydou[1], M. Rospabé[2], G. Ceuleneer[2], B.L. Ehlmann[3,4], E. Leask[3], R.N. Greenberger[3,4], M. Benoît[2],
[1]Institut de Recherche en Astrophysique et Planétologie (Toulouse - France, patrick.pinet@irap.omp.eu), [2]GET (Toulouse, France),
[3]Caltech (Pasadena, CA, USA), [4]Jet Propulsion Laboratory, California Institute of Technology (Pasadena, CA, USA).

1. Introduction and Objectives

The Maqsad area of the Oman ophiolite has been previously documented through an airborne hyperspectral survey [e.g., 1,2,3,4]. One major output resulted in the clear regional delineation of the Moho contact between crust and mantle units (**Figures 1.a, 1.b, 1.c**) .

The present study focuses on a majestic landscape (**Figure 2**) where a wide diversity of mafic ultramafic lithologies is exposed and where the primary igneous stratigraphy of the mantle/crust boundary (oceanic "Moho") is perfectly preserved. Its location is shown on **Figure 1** by means of the black triangle which indicates the approximate field of view; yellow markers highlight the instrument position and main summit seen in the central part of the panorama. A 150m-thick horizon of dunite (made of almost pure, partly serpentinized olivine) is sandwiched between altered mantle harzburgite (olivine + opx) at the bottom and interlayered wehrlites (olivine + cpx) and olivine gabbros on the summits [5].

The objectives are to assess:

-i) the potentiality of in situ hyperspectral survey for landscape lithology mapping and mineralogical reconnaissance versus field groundtruthing,

-ii) how airborne and in situ hyperspectral observation acquired with different resolution and geometry are complementary and can be linked for integrated studies.

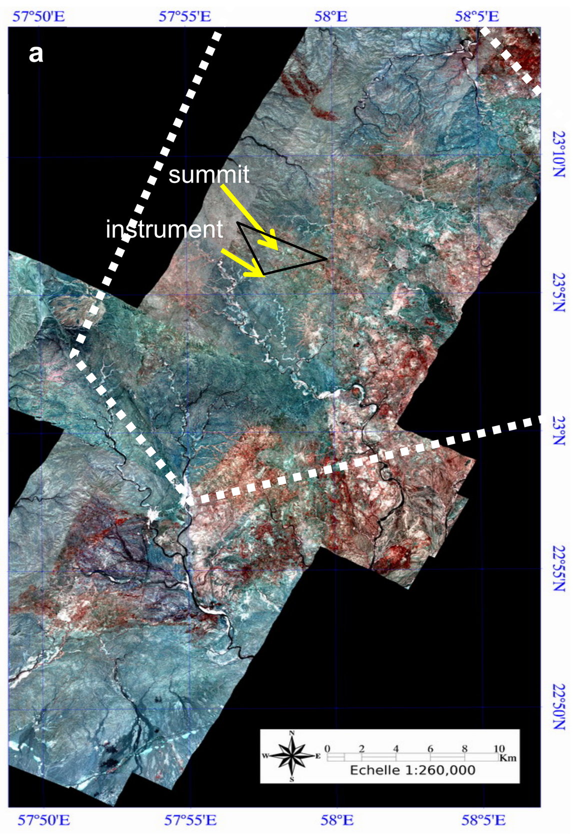

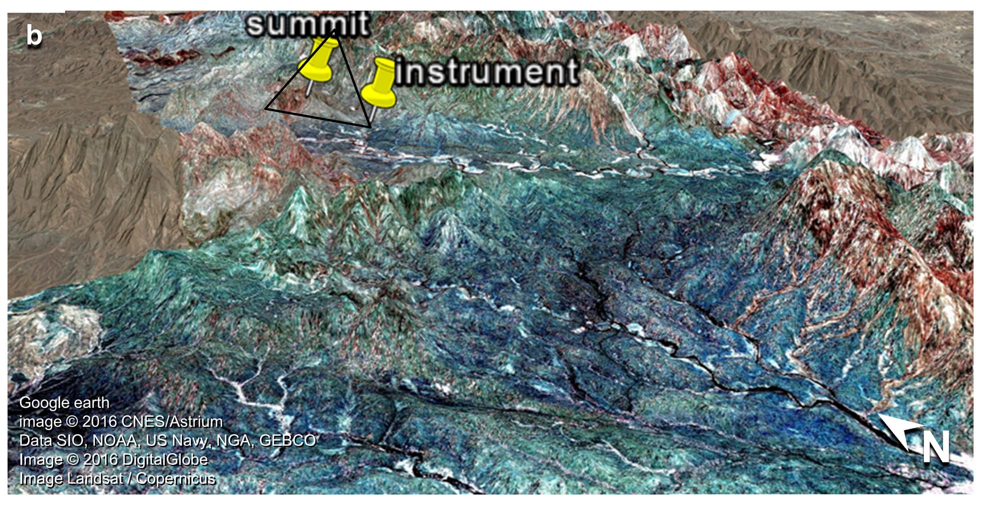

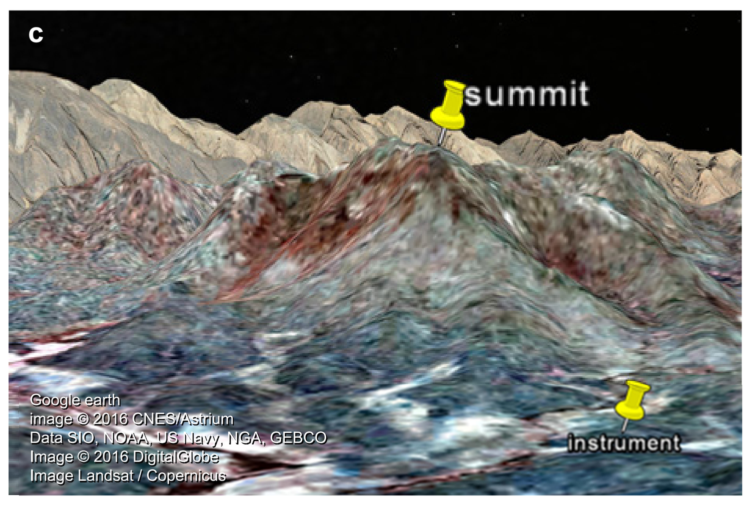

◄ **Figure 1.a** (nadir-looking view) : white dotted outline delimits the field of view shown on Figure 1.b ▲ **Figures 1.b, 1.c** (3D oblique renditions at two different scales over Google earth display) : Spectral RGB composite image derived from HYMAP mosaic at 12 m/pixel. R: 0.87/0.74, G: 0.98/0.74 and 1.03/0.74 µm ratios. Where the contributions of olivine (ol) and orthopyroxene (opx) are weak, and that of clinopyroxene (cpx) is dominant, the absorption feature is strong in the 0.98 µm and 1.03 µm channels resulting in high 0.87/0.74 µm ratio values, low 0.98/0.74 and 1.03/0.74 µm ratio values. Consequently, red-brownish colors correspond to crustal lithologies with the highest cpx content (gabbros, clinopyroxenites, wehrlites) while green-blue colors correspond to ol/ol-opx –rich mantle lithologies (dunites, harzburgites …). Black triangle on **Figures 1.a, 1.b** indicates the approximate field of view of the in situ hyperspectral study; yellow markers highlight the geographic locations of the instrument and main summit seen in the central part of the panorama (see **Figure 2**).

2. Instrument description / data acquisition / field campaign

The Caltech imaging spectrometer system [6] is field-portable. It consists of a quad-core processor and two sensors (f/2.5 aperture vertical slit cameras), co-boresighted on an optical bench. The visible-near infrared (VNIR) sensor acquires data over a spectral range of 0.4-1.0 µm with a 2560x2160 pixel CMOS array with a spectral resolution of 5 nm (FWHM) and a sampling of 1.625 nm. The shortwave infrared (SWIR) sensor acquires data over a spectral range of 0.97-2.60 µm with a 640x512 pixel Stirling-cooled MCT focal plane camera with spectral resolution 6 nm and sampling interval 6 nm (FWHM). The signal-to-noise ratio (SNR) is >100 over all channels. Images are built one image line at a time, viewing the scene through a slit. The system operates in macroscopic mode, using a tripod for imaging of large features, with a fine motion-control rotational stage to acquire panoramic images. The instrument scans over distances of ~7 m to infinity at a single focus. The effective instantaneous field-of-view (IFOV) on target is 0.6 (3) cm (VNIR) and 1.7 (8.5) cm (SWIR), respectively, from a standoff distance of 20 (100) m, with the resolution varying with distance to the outcrop. Scan rates are typically on the order of 1-2°/second, depending on the lighting conditions and resulting exposure times. Exposure times are set manually and optimized to obtain maximum signal without saturating on the brightest scene elements. Dark current and flat field corrections are performed on each image to correct for instrumental effects. Calibration panels are placed in the scene for radiometric/atmospheric correction. During the test field campaign which took place on 2016, January, 9th-22nd, several acquisitions of the scene have been acquired under different conditions and are currently under processing (**Figure 2**).

▲ **Figure 2 :** The hyperspectral acquisition was acquired over a very wide panorama (~180° in azimuth); we analyze here the lithological variability (see sections 1 and 3 for analysis across a subframe (~120° in azimuth) comprised between the vertical hatched lines in white. White small square to the left of the scene corresponds to the spectralon panel used for calibration. The mountain top in the central part of the image corresponds to the summit indicated in **Figure 1**.

3. Image Processing and Preliminary Results

A first step is co-registration of the VNIR channels over the SWIR ones throughout the whole scene of observation, leading to a 0.55-2.45 µm cube, with a 5-6 nm sampling. The pixels are then binned by a factor of 2 in order both to minimize any leftover residual misregistration effect and to increase the SNR. The resulting spatial scale of the spectral investigation of the outcrops is thus on the order of 0.18 (1.8) m at 100 (1000) m distance, which is the typical range within the scene. This scale of analysis represents a significant improvement in resolution over airborne/ spaceborne hyperspectral survey (~6-20m/pixel), extending the capability for the mineralogy / petrology mapping purposes of the outcrops [e.g., 5].

The next step is an attempt at correcting atmospheric effects. The QUAC algorithm has been tested but it requires more knowledge than expected as the atmospheric path for the line of sight is basically horizontal and not nadir-looking. Progress in terms of atmospheric correction are still awaiting. After masking the sky portion of the scene and the highly shadowed or vegetated patches across the scene, a heuristic approach has been implemented here, based on a PCA analysis of the dimensionless dataset (centered coordinates), in the scaled reflectance space for minimizing the photometric effects associated with the variation of lighting and geometry conditions across the scene (**Figure 3**). We notice that the variability is driven along the 1st principal axis (x-axis) by photometric effects, involving topographic slope and backlight geometry and along the 3rd principal axis (y-axis) by a distance factor (related to the optical path through the atmosphere) to the detector (**Figure 3**); this is used for renormalizing the spectral information to a standard distance which corresponds approximately to the distance of the spectralon calibration panel, in the direction of the main summit.

The channels in the atmospheric windows are then discarded and the resulting set is used for exploring the mineralogical variability across the scene. This is performed by means of a clustering analysis in the PC space based on a multidimensional neighborhood approach. The first three principal axes encompass more than 80% of the total variance, with 39.6, 27.4, 13.4% respectively, and a significant drop to 2.3 , 1.9% and less than 1% occurs for the next axes.

As a result, a first-order lithological mapping (**Figure 4**) of the landscape is produced, mainly driven by variable mafic absorptions in the 1 µm domain in agreement with [1,2,3,7].

However, one clear difference is found between airborne and in situ derived mapping products for the forefront part of the scene. The in situ observation (oblique grazing geometry, (sub)metric scale resolution) is able to pick out together the forefront quaternary deposits of gabbro boulders and exposed upsection interlayered gabbros / wehrlites (pink cluster in **Figure 4**) where the airborne observation (nadir-looking geometry, decameter scale resolution) maps the forefront unit as a harzburgitic field (blueish-greenish color in **Figure 1.c**). **It is worth to point out that both are actually right : it just means that under grazing geometry conditions the harzburgitic substrate in the forefront is masked by the gabbro boulders on top while these boulders are hardly detected at lower resolution under nadir-looking geometry**. The groundtruth based on field work is here decisive to grasp the situation.

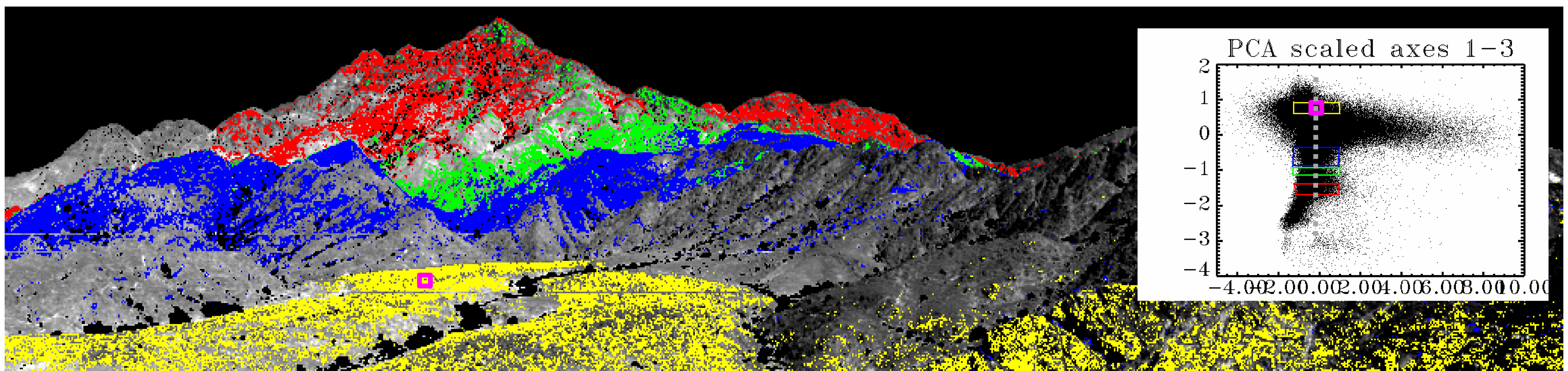

▲ **Figure 3 :** Color units across the scene are associated with the same color rectangles in the PC space sampling the y-axis, displayed by the grey-dashed line; Pink square corresponds to the reference location used for renormalizing the spectral information across the scene, approximately taken at the same distance as the spectralon panel (which is actually to the left of the complete scene) (see **Figure 2**).

Figure 5 ► : Field work section (~500 m of vertical extent) [5]. Bottom to top: Red and light green squares: harzburgite outcrops; dark blue and yellow: dunite unit; cyan: cpx dunite outcrop; pink and dark green: wehrlite and gabbro outcrops.

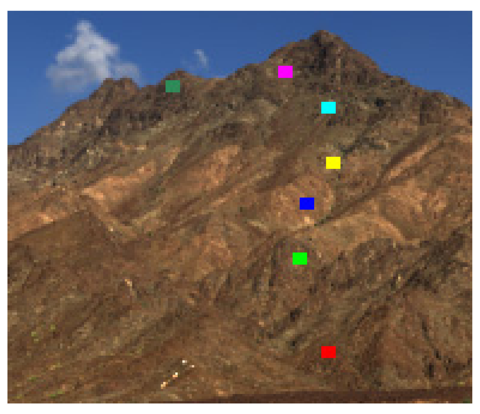

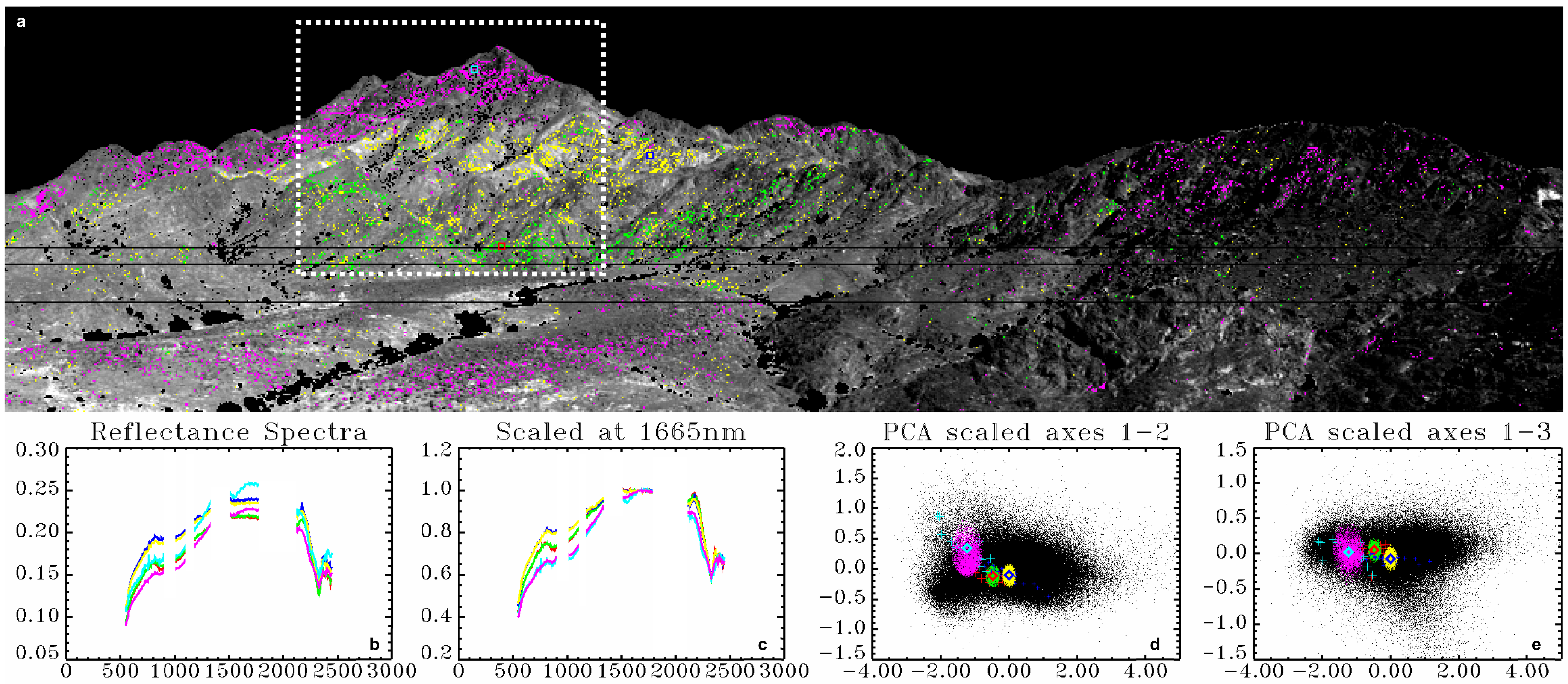

▲ **Figure 4 :** First-order mineralogical mapping (a) derived from a PC space clustering analysis (d, e), white dotted frame for location of Fig.5. cyan (reference) and pink (cluster) spectra (b: reflectance, c: reflectance scaled at 1665 nm; wavelength on both plots in nm) and distribution (d,e) highlight forefront quaternary deposits of gabbro boulders and exposed upsection interlayered gabbros / wehrlites; dark blue (reference) and yellow (cluster) spectra (b, c) and distribution (d, e) display dunitic exposures; red (reference) and green (cluster) spectra (b, c) reveal harzburgite outcrops. The 2 µm domain is dominated by an ubiquitous 2.3 µm absorption feature (carbonate /serpentinization effects) and hydroxyl group (OH) features at 2.13 and 2.25 µm.

4. Implications and future steps

The results produced here demonstrate the great potentiality of hyperspectral survey for landscape lithology mapping and mineralogical reconnaissance both for *terrestrial and planetary in situ exploration*; it also highlights possible intricacies not to be overlooked for the sake of interpretation.

The in situ submetric scale of analysis represents a clear improvement in resolution over airborne/ spaceborne hyperspectral survey (~6-20 m / pixel), extending the capability for the mineralogy / petrology mapping purposes [e.g., 5].

More investigations of this kind must be performed to improve our skills in combining orbital / in situ spectral observations on Mars (e.g., CRISM (MRO) / Mastcam (MSL)) and prepare for Mars-2020.

References

[1] Pinet P.C. et al. (2006) *LPS XXXVII*, Abstract #1346.
[2] Combe J.-P. et al. (2006) *Geochem. Geophys. Geosyst.*, 7, Q08001.
[3] Clenet H. et al. (2010), *Lithos, 114*, 265–281, doi:10.1016/lithos.2009.09.002.
[4] Clenet H. et al. (2013), *JGR Planets, 118*, 1-24.
[5] Rospabé, M. et al. (2017), *Geology*, in press.
[6] Greenberger R.N. et al. (2016) *IEEE Whispers Conf. 8th*, 4p.
[7] Roy, R. et al. (2009) *Geochem. Geophys. Geosyst., 10*, Q02004.

LUNAR AND PLANETARY SCIENCE CONFERENCE 48TH, HOUSTON (THE WOODLANDS), TEXAS, USA, MARCH 20-24, 2017